Eur. Phys. J. Special Topics **227**, 155–166 (2018)

https://doi.org/10.1140/epjst/e2018-00058-6

THE EUROPEAN PHYSICAL JOURNAL SPECIAL TOPICS

Regular Article

A highly effective energy mitigation system combining carbon nanotube and buckyballs

Dayong Hu[1,2,3], Jianxing Hu[2,4], Hanlin Jiang[1,2,3], and Jun Xu[2,4,5,a]

[1] Department of Aircraft Airworthiness Engineering, School of Transportation Science and Engineering, Beihang University, Beijing 100191, P.R. China
[2] Advanced Vehicle Research Center (AVRC), Beihang University, Beijing 100191, P.R. China
[3] Aircraft/Engine Integrated System Safety Beijing Key Laboratory, Beijing 100191, P.R. China
[4] Department of Automotive Engineering, School of Transportation Science and Engineering, Beihang University, Beijing 100191, P.R. China
[5] Beijing Key Laboratory for High-efficient Power Transmission and System Control of New Energy Resource Vehicle, Beihang University, Beijing 100191, P.R. China

Received 28 July 2017 / Received in final form 7 February 2018
Published online 10 September 2018

Abstract. By combining a carbon nanotube with buckyballs, a novel energy dissipation system is investigated for impact protection based on molecular dynamics (MD) simulations. To explore the energy mitigation mechanism of the carbon nanotube with buckyballs system (C_{60}-CNT), four types of C_{60}-CNT systems are considered. Computational results indicate that the deformation of buckyballs and the interaction between buckyballs and carbon nanotube play a critical role for the energy mitigation of C_{60}-CNT system. And results also show that the energy dissipation efficiency of C_{60}-CNT system is higher than water-CNT system, and more than 50% of impact energy can be mitigated. Further, parametric studies are conducted by varying governing factors, including length and diameter of the carbon nanotube, the number of the buckyballs and impacting energy. Results may help to understand the underlying mechanism of C_{60}-CNT system for impact protection, and explore the promising candidates of non-liquid energy mitigation system.

1 Introduction

It is imperative to select advanced materials and design structures for impact protection. Nowadays, conventional materials and structures are far from satisfactory in impact energy dissipation due to the limits of their specified energy absorption capability [1–3]. More and more researchers have turned their focuses to nanoporous materials and structures, and discovered that nanoporous materials and fullerene materials are excellent candidates for impact protection [4–10].

[a] e-mail: junxu@buaa.edu.cn

Systematic studies have been conducted to investigate the energy absorption of nanoporous materials mixed with liquids, i.e. a system named NEAS (Nanoporous Energy Absorption System) [4,5,11,12]. The fundamental working mechanism for a NEAS system is to dissipate hazardous impact energy into extra interfacial energy once the water molecules are forced to infiltrate into a hydrophobic confined nanopore, e.g. carbon nanotube (CNT) [4,5]. On one hand, experimental studies were conducted to firstly observe the counterintuitive nanofluidic behaviors. For example, Han et al. pioneered to prove that the specified energy absorption of nanoporous silica materials mixed with water was on the order of 300 J/g, greater than most of conventional materials and structures and revealed a bright prospect for energy dissipation [13]. Sun et al. conducted low-speed impact experiments based on drop hammer to shed light on the cushioning effect of the zeolite β/water system, which further supported NEAS system as an excellent candidate for damping and impact protection [11]. On the other hand, studies using molecular dynamics (MD) for CNT/water system were extensively conducted [6,14–16]. Cao et al. used MD simulation to illuminate the working mechanism of CNT/water system subjected to external crushing and reveal that the impact velocity and nanotube radius may take an important role on the nanofluidic behavior of water molecules in the CNT [17,18]. Liu et al. employed MD simulations to explore the infiltration behavior of water invading into nanopores under quasi-static condition, and found that applied charges, addition of ions, thermal effects and the construction of nanopore could influence the infiltration behavior and promote or impede the energy mitigation [14,19–21]. Xu et al. further discussed the effects of some major parameters from an engineering perspective, such as impact velocity, nanopore size, and pore composition, on energy mitigation of the system under dynamic condition [15]. Hu et al. took one step further to investigate the energy mitigation mechanism of the heterojunction CNT/water system and revealed that nanopore construction and impact velocity had effects on the energy dissipation [16].

Recently, in addition to the CNT, other fullerenes, such as buckyballs, are also attractive for cushioning and impact protection. Xu et al. investigated the dynamics impact response and energy mitigation properties of the individual buckyball and buckyballs chain, and found that larger buckyballs are competent to mitigate energy due to their non-recoverable deformation [8–10]. Chen et al. put forward energy absorption system comprised of a CNT with nested buckyballs and showed the promising application for impact protection [22].

Inspired by the CNT/water system and CNT nested with buckyballs system, a new energy dissipation system comprised of CNT and C_{60}s is firstly established in the current study. MD simulation is carried out to investigate mechanical behavior and energy dissipation mechanism of C_{60}-CNT system subject to external high energy/speed impact. Further, the effects of impact energy, the size of CNT, and the number of buckyballs are parametrically discussed to provide a systematic guidance for possible system tuning.

2 Computational model and method

The computational model is comprised of a receiver, an impactor, a rigid carbon nanotube with length of L_0 and a C_{60} reservoir with multiple C_{60}s, as illustrated in Figure 1. The left end of the CNT is closed to prevent C_{60}s from flowing out of the CNT, while the right end is open to connect the C_{60} reservoir. The C_{60} reservoir is bounded by two parallel rigid plates, the left plate, fixed to the CNT, has a hole in the center, through which C_{60}s can invade into CNT, while the right plate is used to mimic the piston to be impacted by the impactor. Periodic boundary conditions are

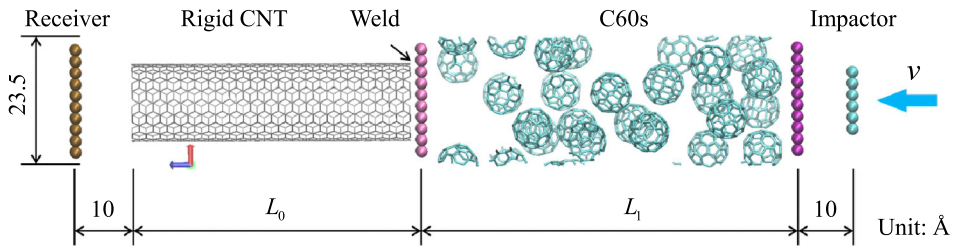

Fig. 1. The model of the C_{60}-CNT energy dissipation system.

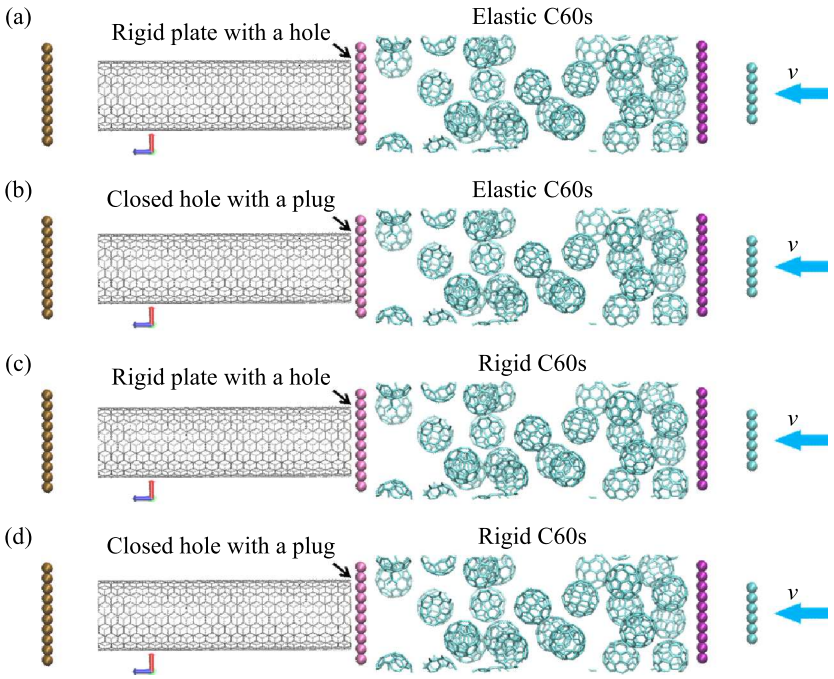

Fig. 2. Four different C_{60}-CNT systems: (a) System-1; (b) System-2; (c) System-3; (d) System-4.

employed for the lateral directions to eliminate the boundary effects. The impactor and receiver are modeled by two rigid mass. When the system is impacted by the impactor, a compressive wave forms and propagates towards to the receiver from right of system, which causes C_{60}s deformation and infiltration, buffering a large amount of impact energy. When the system collides the receiver, the transmitted force will be recorded. Subsequently, the impactor rebounds back and releases the stored potential energy. For convenience to compare, the C_{60}-CNT system is marked as System-1, three comparison systems are also established as shown in Figure 2. System-2 has the identical characteristics as System-1 except that the right end of CNT is closed with a plug. System-3 and System-4 are based on System-1 and System-2 with the substitution of rigid C_{60}s, respectively.

MD simulations are carried out based on LAMMPS (large-scale atomic/molecular massive parallel simulator), developed by Sandia National Laboratory [23]. And the 12-6 Lennard-Jones (L-J) empirical force field is employed to depict the intermolecular

potential between atoms as follows:

$$U(r_{ij}) = 4\varepsilon \left[\left(\frac{\sigma}{r_{ij}} \right)^{12} - \left(\frac{\sigma}{r_{ij}} \right)^{6} \right], \tag{1}$$

where r_{ij} is the distance between atoms, ε is the well depth of the potential, and σ is related to the equilibrium distance between atom-i and atom-j. The parameters of L-J potential between carbon atoms are $\sigma = 0.340$ nm and $\varepsilon = 0.0860$ kcal/mol [24]. The cutoff distance for the intermolecular interaction is set to be 1.0 nm. The buckyballs in the C_{60} reservoir firstly are placed in an orderly arrangement, then equilibrated for 40 ps using a canonical ensemble (NVT). The Nose–Hoover thermostat is used to keep a temperature of 300 K. By employing the aforementioned L-J potential, the suction will not occur during the relaxation progress. After equilibration, a micro-canonical ensemble (NVE) is employed to simulate the impact process. The total simulation time of 100 ps and a time integration step of 1 fs are adopted.

3 Results

At a representative impact speed of 250 m/s, the deformation sequences for System-1 nominated C_{60}-(10,10)CNT-L5.0-24, ((10,10) and 5.0 represent diameter and length of CNT, and 24 is the buckyball number), are illustrated in Figure 3. When the impactor strikes the piston, the system moves left and impacts the receiver, accompanied with that buckyballs are compacted and then invaded into the CNT at $t = 14$ ps. Infiltration phenomenon in C_{60}-CNT system could not be observed, which means that the repulsive force between CNT and C_{60}s is not remarkable. It is noted that the C_{60}s, invaded into CNT, have not visible deformation. At $t = 21$ ps, the C_{60}s in C_{60}s reservoir are highly compacted and significantly deformed. And the C_{60}s in CNT begin to show larger compression because more and more C_{60}s are invaded at $t = 26.5$ ps. When $t = 35$ ps, the entire system and impactor has begun to bounce back. Finally, all the deformation of C_{60}s recover fully and 5 C_{60}s are left in the CNT. During the process, the impact energy converts into kinetic energy of C_{60}s and potential energy because of deformation and the interactions between C_{60}s and CNT, as shown in Figure 4a.

Deformation of the buckyballs in System-2 is larger than System-1 during the impact. This can be explained by that the buckyballs cannot be infiltrated into CNT and suffer more impact energy from the impactor such that a larger potential energy value is observed because of a serious deformation of buckyballs. However, the potential energy would release and convert into the kinetic energy of impactor when the impactor bounces back as shown in Figure 4b. If C_{60}s are set to be rigid, the energy mitigation mechanism is that the impact energy will convert into kinetic energy of system during the impact process as shown in Figure 4c and d for System-3 and System-4, respectively. The above comparisons indicate that the deformation of the buckyballs and the interaction between the buckyballs and carbon nanotube play a critical role for the energy dissipated of C_{60}-CNT system.

4 Discussion

To discuss the mitigation performances of energy and impact force for the C_{60}-CNT system, two parameters are adopted. Energy dissipation efficiency, $\eta = \Delta E_{\mathrm{k}}/E_{\mathrm{Impact}} \times 100\%$, and the reduction of transmitted force, $\Delta F = (F'_{\max} - F_{\max})/F'_{\max} \times 100\%$; where ΔE_{k} is reduction of impact energy, E_{Impact} is impact

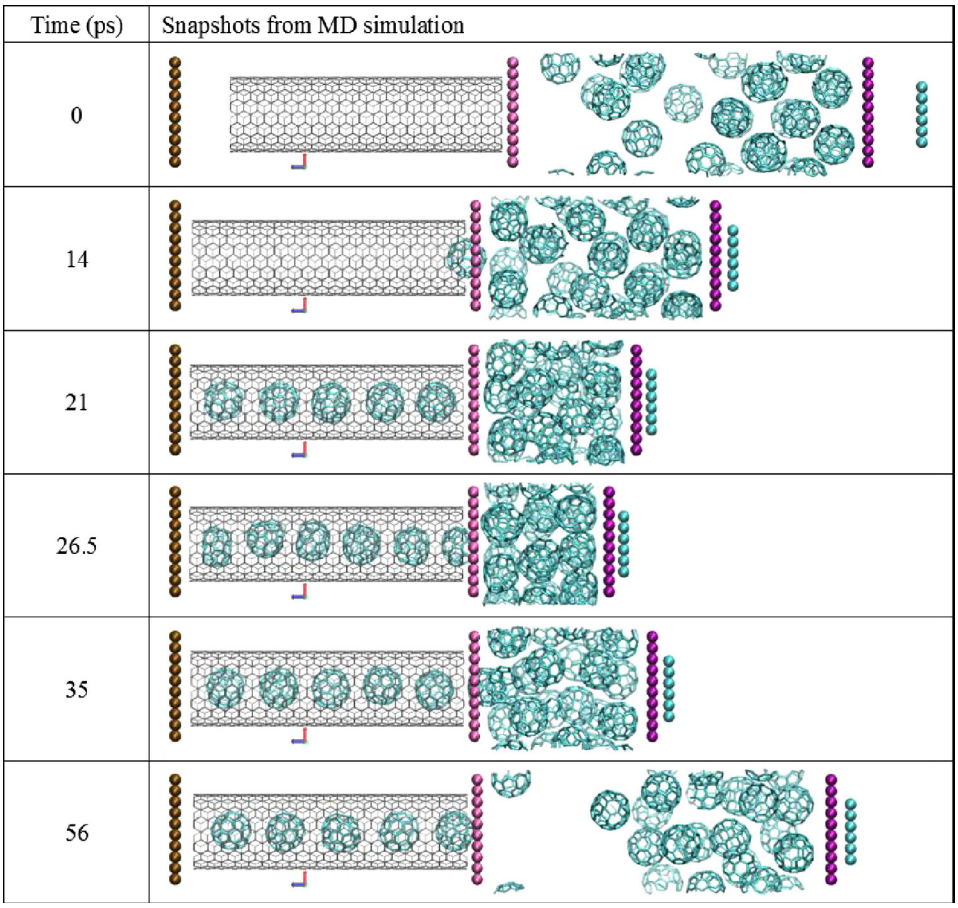

Fig. 3. Sequences of deformation for System-1 (C_{60},-(10,10)CNT-L5.0-24).

energy, $F_{\max}$ is the maximum force of C_{60}-CNT system, and $F'_{\max}$ is the maximum force of its comparison systems. In addition, specific energy absorption (SEA), defined as SEA $= \int_0^w F(x)\,\mathrm{d}x/M$, is used to quantify the energy dissipation capability of the system [25]; where M is the total mass of C_{60}-CNT system.

4.1 The effect of impact velocity

Considering C_{60}-CNT system as the representative system, the simulations with impact velocities varying from 50 m/s to 600 m/s are carried out. Figure 5 shows the energy dissipation efficiency of the C_{60}-CNT system and its comparison systems. The energy dissipation efficiency has a trends of decreasing but less than 20% as the impact velocity increases, which indicates the energy mitigation capability of the C_{60}-CNT systems keep a stable level at various impact energy. When the impact velocity increase, more impact energy converts into the kinetic energy and potential energy of the system. Meanwhile, Figure 5 also depicts that System-1 has the better energy dissipation efficiency, System-2 without the infiltration of C_{60}s could dissipate more energy compared to System-3 and System-4 with rigid buckyballs, indicating

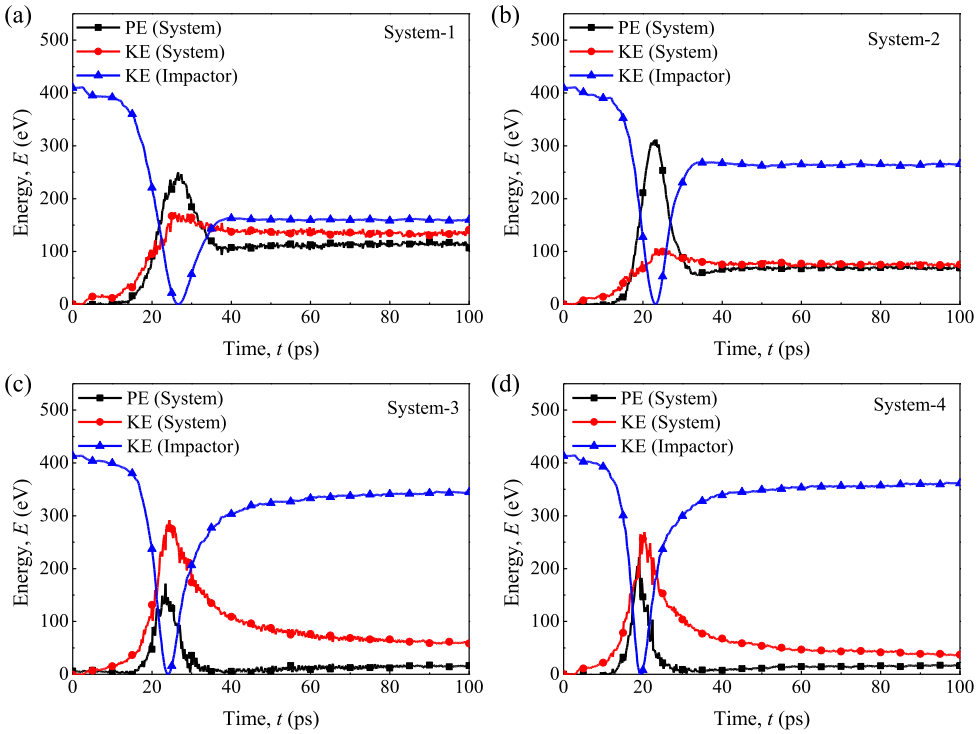

Fig. 4. Energy conversion situation for C_{60}-CNT system and its comparison systems.

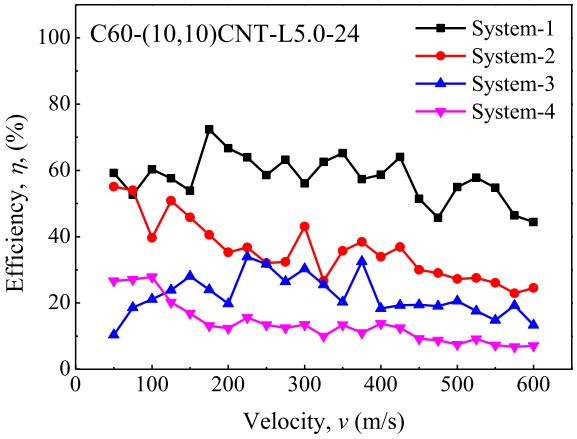

Fig. 5. The energy dissipation efficiency of C_{60}-CNT system and its comparison systems under various impact velocities.

that the infiltration of buckyballs and the deformation of C_{60}s play an important roles for impact protection.

It is noted that buckyballs would be totally crushed when the impact velocity exceeds 600 m/s, so that the energy absorption efficiency of C_{60}-CNT system will not increase any more. Therefore, the higher velocity is not considered here. In current study, more impact energy is dissipated with impact velocity increase, which indicates that specified energy absorption (SEA) of the system is highly related to the impact

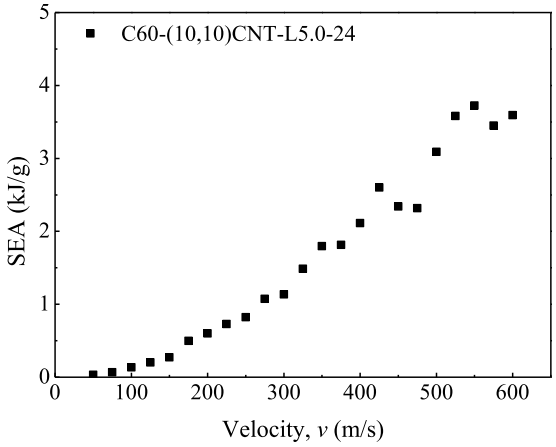

Fig. 6. Specified energy absorption of the C_{60}-CNT system under different velocities.

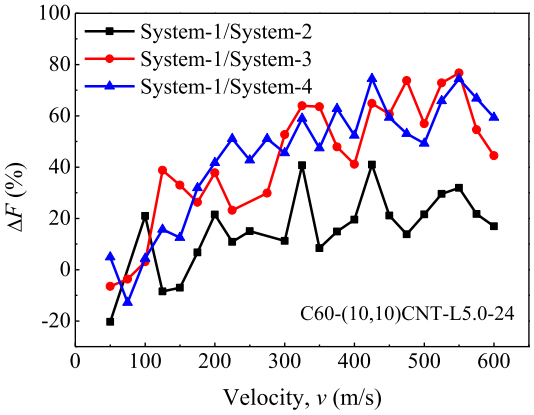

Fig. 7. The transmitted force reduction under different impact velocities for the comparison systems of the C_{60}-CNT.

velocity, as shown in Figure 6. The SEA value increases with the impact velocity, and it reaches up to 1.13 kJ/g at the velocity of 300 m/s, which means a great prospect for impact protection.

The transmitted force reduction, ΔF, is also given in Figure 7. The result of System-1/System-2 indicates that the infiltration of buckyballs almost has no influence on the force mitigation at the low velocity. The small number of infiltrated buckyballs can be used to explain this phenomenon. The peak force of System-1 is smaller compared with System-3 and System-4 at a higher velocity, even the ΔF reaches 40–60% when the velocity varies from 300 m/s to 600 m/s. Which illustrates that the deformation of buckyballs play a critical role in force reduction at a high impact velocity.

4.2 The effect of CNT length

In general, nanotube length may affects the nanopore volume of storing potential energy during impact, this phenomenon has been reported for the water-CNT system [15,16]. In this section, C_{60}-(10,10)CNT-24 systems with different CNT

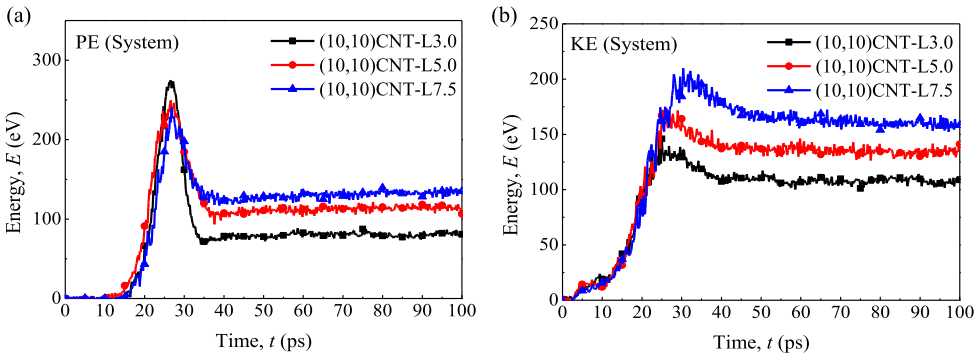

Fig. 8. Energy conversion for C_{60}-CNT system with different CNT length: (a) potential energy; (b) kinetic energy.

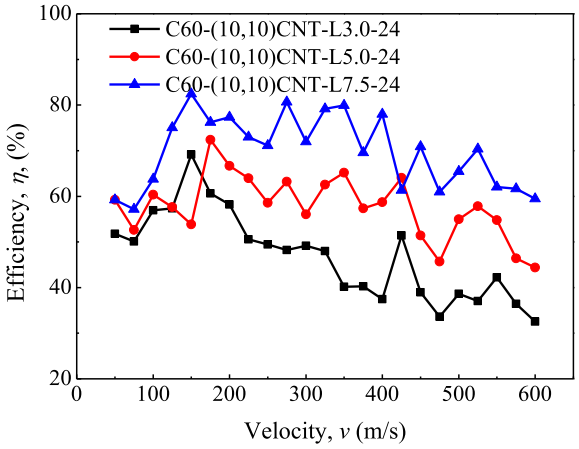

Fig. 9. The energy dissipated efficiency of C_{60}-CNT systems with different CNT length under various impact velocities.

lengths ($L_0 = 3.0$, 5.0, 7.5 nm) are established and the energy mitigation efficiency is elaborated.

The elongation of the carbon nanotube facilitates the interaction between C_{60}s and CNT, which makes more impact energy converted into potential energy and kinetic energy, as shown in Figure 8. Figure 9 depicts the variation of energy mitigation efficiency with impact velocity for different carbon nanotube lengths. The energy mitigation efficiency increases apparently with the carbon nanotube length under various impact velocities. Particularly, at the same impact velocity of 300 m/s, $\eta = 49.1\%$ for C_{60}-(10,10)CNT-L3.0-24 and $\eta = 71.9\%$ for C_{60}-(10,10)CNT-7.5-24.

To sum up, the invasion of buckyballs has no effect on the force mitigation, which is dominated by the deformation of buckyballs. When elongate the carbon nanotube, only can one or two more C_{60}s infiltrate into CNT, which in fact has no significant difference in transmitted force with initial system, as shown in Figure 10.

4.3 The effect of CNT diameter

Similar to the effect of CNT length, CNT diameter also affects the nanopore volume to storing potential energy [15]. Here, C_{60}-(n, n)CNT-L5.0-24 systems ($n = 10$,

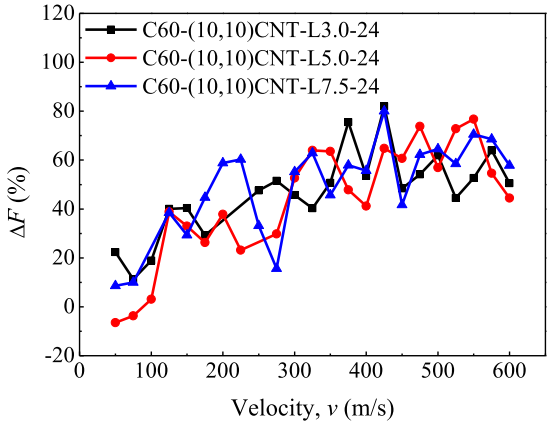

Fig. 10. The transmitted force reduction with different CNT length under different impact velocities.

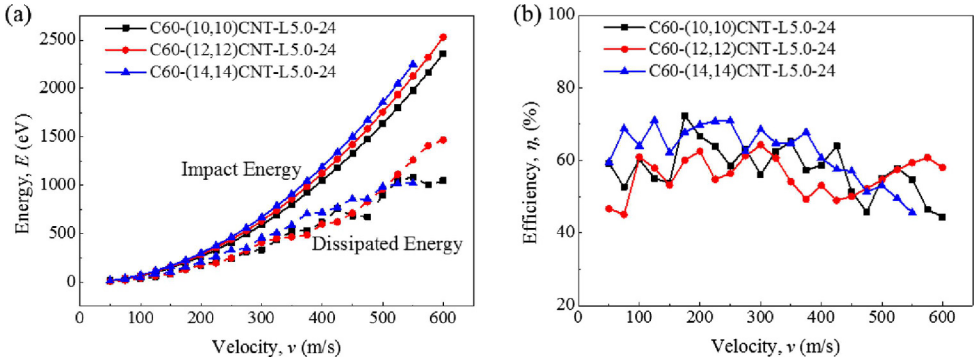

Fig. 11. C_{60}-CNT system with different CNT diameter: (a) the various impact energy and corresponding dissipated energy; (b) the energy dissipated efficiency.

12, 14) are established and the diameter of the hole in the center of the left rigid plate connected to the buckyballs reservoir is also equal to diameter of CNT to discuss the effect of CNT diameter on the energy mitigation efficiency and transmitted force reduction. It is noted that the C_{60}-CNT system is different from water-CNT system, the size of water molecule compared with nanopore is sufficient small, while the buckyballs are large and the diameter is close to that of CNT, which leads to the different results compared with water-CNT system [15]. For water-CNT system, more water molecules can be infiltrated into the CNT with larger diameter. However, for C_{60}-CNT system, only a few buckyballs may be left in the CNT during impact process. For instance, 5 buckyballs for C_{60}-(10,10)CNT-L5.0-24 system and 7 buckyballs for C_{60}-(14,14)CNT-L5.0-24 system under the impact velocity of 250 m/s, which indicates that the dissipated energy keep a stable level when various CNT diameters, as shown in Figure 11a. Figure 11b shows the energy mitigation efficiency at various CNT diameters, and it is obvious that the increase of CNT diameter cannot improve the energy mitigation like CNT/water systems.

Similar to the effect of nanotube length, the increase of CNT diameter here cannot store more buckyballs, because the CNT diameters, ranging from 1.36 nm to 1.90 nm, are close to the buckyball diameter of 0.71 nm. Which indicates that the transmitted

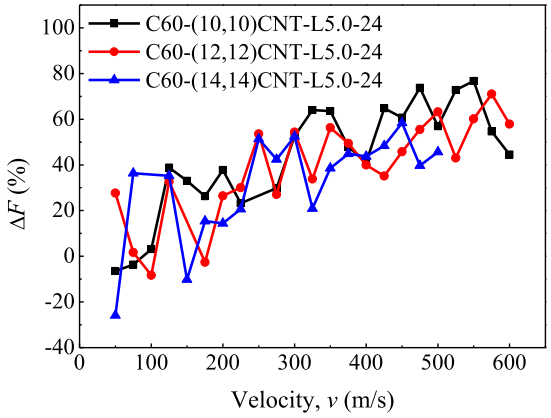

Fig. 12. The transmitted force reduction of C_{60}-CNT systems with different CNT diameters under various impact velocities.

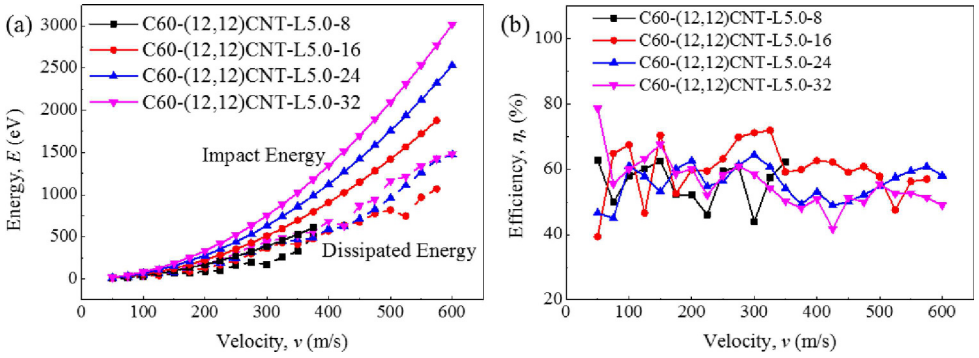

Fig. 13. C_{60}-CNT system with different buckyball number: (a) the various impact energy and corresponding dissipated energy; (b) the energy dissipated efficiency.

force reduction of C_{60}-CNT would keep a stable level with varying CNT diameters when identical impact velocity, as shown in Figure 12.

4.4 The effect of buckyballs number

When designing C_{60}-CNT system, the number of the buckyball is considerable. The buckyballs deformation could not play a remarkable role for energy dissipation and great transmitted force will be caused because of two rigid plate collision when there is no sufficient buckyballs to fill the nanopores of system. Taking C_{60}-(12,12)CNT-L5.0 with different buckyball numbers (8, 16, 24, 32) as the representative systems, various impact velocities ranging from 50 m/s to 600 m/s are adopted. Figure 13a gives the impact energy (solid lines) and dissipated energy (dash lines) of these systems. When the system just has 8 buckyballs, it cannot normally work at a higher impact velocity because most of buckyballs are invaded into the CNT. The remaining buckyballs extremely deform and two rigid plates collide, resulting in the great transmitted force. Therefore, there must be adequate buckyballs to make the system work. It is noted that the system still is effective at a higher impact velocity with the buckyballs increase, as shown in Figure 13b. However, the dissipated energy efficiency keeps a stable level as buckyballs increase under different impact velocities.

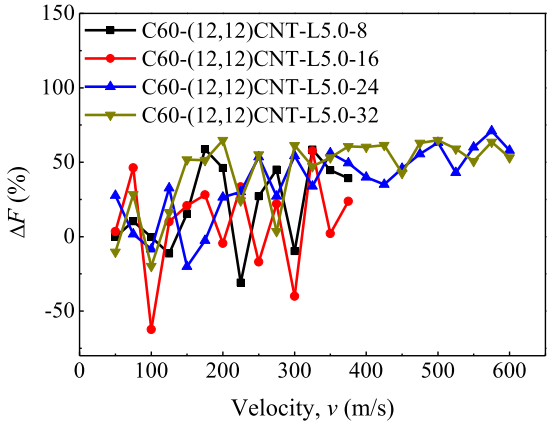

Fig. 14. The transmitted force reduction of C_{60}-CNT with different buckyball number under various impact velocities.

As the buckyball number increase to 24 or 32, the number of invaded buckyballs is still the same, and the averaging impact energy of each buckyball is similar for both systems at the same impact velocity, so the transmitted force reduction is also approximately the same as shown in Figure 14.

5 Concluding remarks

The C_{60}-CNT energy mitigation system combining carbon nanotube with buckyballs for impact protection is established and explored based on LAMMPS (large-scale atomic/molecular massive parallel simulator). When the system is impacted by an impactor, the buckyballs in C_{60} reservoir will be highly compressed and invaded into CNT, converting the impacting energy into kinetic energy of buckyballs and excessive surface energy of the system because of the elastic deformation of C_{60}s and the interactions between C_{60}s and CNT, and reducing the transmitted energy and force to the receiver. Three comparison systems are also established and discussed to investigate the energy mitigation mechanism of C_{60}-CNT systems. Results indicate that the deformation of C_{60}s and the interaction between C_{60}s and CNT are dominated. The transmitted force mitigation of the C_{60}-CNT system is dominated by the deformation of C_{60}s, and more than 50% force could be mitigated compared to its comparison systems with rigid C_{60}s. However, the interaction between C_{60}s and CNT have no distinct difference for transmitted force mitigation. Further, parametric analysis is performed by varying governing factors, including impact energy, CNT length, CNT diameter and C_{60} number. These results indicate that the energy dissipation of the C_{60}-CNT system is related to the dimensions of the CNT and the impact energy. The C_{60}-CNT system may be effective in a large range of impact velocities.

Results may pave the road to understand the energy mitigation mechanism of the C_{60}-CNT system and help to design the nano-device for impact protection.

JX and DH would like to thank for the Natural Science Foundation of China (Grant No. U1664250), Beihang University and Beijing Municipal Science & Technology Commission (Grant No. Z161100001416006). DH would like to thank for the funding support from Defense Industrial Technology Development Program (JCKY2016601B001).

Author contribution statement

JX conceived and designed the study. HJ, JH performed the simulations. Analyzed the data: HJ, JH, DH and JX. HJ, JH DH and JX wrote the paper.

References

1. X.M. Qiu, T.X. Yu, Appl. Mech. Rev. **65**, 024001 (2012)
2. G.Y. Lu, Z.J. Han, J.P. Lei, S.Y. Zhang, Thin-Walled Struct. **47**, 1557 (2009)
3. S.H. Chen, K.C. Chan, F.F. Wu, L. Xia, Sci. Rep. **5**, 10302 (2015)
4. X. Kong, Y. Qiao, Appl. Phys. Lett. **86**, 151919 (2005)
5. A. Han, Y. Qiao, Langmuir **23**, 11396 (2007)
6. X. Chen, G. Cao, A. Han, V.K. Punyamurtula, L. Liu, P.J. Culligan, T. Kim, Y. Qiao, Nano Lett. **8**, 2988 (2008)
7. Y. Qiao, L. Liu, X. Chen, Nano Lett. **9**, 984 (2009)
8. J. Xu, Y. Li, Y. Xiang, X. Chen, PLoS ONE **8**, e64697 (2013)
9. J. Xu, Y. Li, Y. Xiang, X. Chen, Nanoscale Res. Lett. **8**, 1 (2013)
10. J. Xu, Y. Sun, B. Wang, Y. Li, Y. Xiang, X. Chen, Mech. Res. Commun. **49**, 8 (2013)
11. Y. Sun, Z. Guo, J. Xu, X. Xu, C. Liu, Y. Li, Mater. Des. **66**, 545 (2015)
12. W. Lu, *Novel protection mechanism of blast and impact waves by using nanoporous materials* (Springer International Publishing, 2016)
13. A. Han, V.K. Punyamurthula, W. Lu, Y. Qiao, J. Appl. Phys. **103**, 084318 (2008)
14. L. Liu, X. Chen, W. Lu, A. Han, Y. Qiao, Phys. Rev. Lett. **102**, 184501 (2009)
15. B.X. Xu, Y. Qiao, X. Chen, J. Mech. Phys. Solids **62**, 194 (2014)
16. D. Hu, H. Jiang, K. Meng, J. Xu, W. Lu, Phys. Chem. Chem. Phys. **18**, 7395 (2016)
17. G. Cao, Y. Qiao, Q. Zhou, X. Chen, Mol. Simul. **34**, 1267 (2008)
18. H. Liu, G. Cao, J. Chem. Phys. **139**, 114701 (2013)
19. L. Liu, Y. Qiao, X. Chen, Appl. Phys. Lett. **92**, 101927 (2008)
20. L. Liu, J. Zhao, P.J. Culligan, Y. Qiao, X. Chen, Langmuir **25**, 11862 (2009)
21. L. Liu, J.B. Zhao, C.Y. Yin, P.J. Culligan, X. Chen, Phys. Chem. Chem. Phys. **11**, 6520 (2009)
22. H. Chen, L. Zhang, M.D. Becton, H. Nie, J. Chen, X. Wang, Phys. Chem. Chem. Phys. **17**, 17311 (2015)
23. S. Plimpton, J. Comput. Phys. **117**, 1 (1995)
24. G. Hummer, J.C. Rasaiah, J.P. Noworyta, Nature **414**, 188 (2001)
25. G. Lu, T.X. Yu, *Energy absorption of structures and materials* (Woodhead Publishing, Cambridge, 2003)